Rapid and active stabilization of visual cortical firing rates across light–dark transitions

Alejandro Torrado Pacheco[a,1], Elizabeth I. Tilden[a,1,2], Sophie M. Grutzner[a,1,3], Brian J. Lane[a], Yue Wu[b], Keith B. Hengen[a,2], Julijana Gjorgjieva[b,c], and Gina G. Turrigiano[a,4]

[a]Department of Biology, Brandeis University, Waltham, MA 02453; [b]Computation in Neural Circuits Group, Max Planck Institute for Brain Research, 60438 Frankfurt, Germany; and [c]School of Life Sciences, Technical University of Munich, 85354 Freising, Germany

Contributed by Gina G. Turrigiano, June 18, 2019 (sent for review April 17, 2019; reviewed by Chinfei Chen and Cristopher M. Niell)

The dynamics of neuronal firing during natural vision are poorly understood. Surprisingly, mean firing rates of neurons in primary visual cortex (V1) of freely behaving rodents are similar during prolonged periods of light and darkness, but it is unknown whether this reflects a slow adaptation to changes in natural visual input or insensitivity to rapid changes in visual drive. Here, we use chronic electrophysiology in freely behaving rats to follow individual V1 neurons across many dark–light (D-L) and light–dark (L-D) transitions. We show that, even on rapid timescales (1 s to 10 min), neuronal activity was only weakly modulated by transitions that coincided with the expected 12-/12-h L-D cycle. In contrast, a larger subset of V1 neurons consistently responded to unexpected L-D and D-L transitions, and disruption of the regular L-D cycle with 60 h of complete darkness induced a robust increase in V1 firing on reintroduction of visual input. Thus, V1 neurons fire at similar rates in the presence or absence of natural stimuli, and significant changes in activity arise only transiently in response to unexpected changes in the visual environment. Furthermore, although mean rates were similar in light and darkness, pairwise correlations were significantly stronger during natural vision, suggesting that information about natural scenes in V1 may be more strongly reflected in correlations than individual firing rates. Together, our findings show that V1 firing rates are rapidly and actively stabilized during expected changes in visual input and are remarkably stable at both short and long timescales.

visual experience | rodent vision | visual cortex | firing-rate stability

Neurons in the cerebral cortex are spontaneously active, but the function of this internally generated activity is largely unexplained. Ongoing activity has been proposed to be noise due to random fluctuations (1–3). However, other experiments have shown that spontaneous activity possesses coherent spatiotemporal structure (4–6), suggesting that it may play an important role in the processing of natural sensory stimuli (4, 7–11). In primary visual cortex (V1), spontaneous activity observed in complete darkness is similar to that evoked by visual stimulation with random noise stimuli and is only subtly modulated by natural scene viewing (8, 12). Recently, we showed that individual V1 neurons have very stable mean firing rates in freely behaving rodents and that these mean rates are indistinguishable in light and dark when averaged across many hours (13). How V1 firing can be stable across such drastic changes in the visual environment while still meaningfully encoding sensory stimuli and whether this stability is actively maintained or simply arises from intrinsic circuit dynamics remain unknown.

Regulation of individual firing rates around a stable set point is thought to be essential for proper functioning of cortical circuits in the face of developmental or experience-dependent perturbations to connectivity (14, 15). Long-term stability of individual mean firing rates has now been observed in rodent V1 (13, 16, 17) and primary motor cortex (18), suggesting that it is a general feature of neocortical networks; furthermore, perturbing V1 firing rates through prolonged sensory deprivation results in a slow but precise homeostatic regulation of firing back to an individual set point, showing that neurons actively maintain these set points over long timescales (13). This stability in mean firing rates, even across periods of light and dark, raises the question of how natural visual input is encoded by V1 activity in freely behaving animals. One possibility is that changes in visual drive result in rapid fluctuations in mean firing rates that operate over seconds to minutes. Another possibility is that firing rates are stabilized even over these short timescales, and visual information is primarily encoded in higher-order network dynamics.

To generate insight into these questions, we followed firing of individual neurons in V1 of freely behaving young rats over several days as animals experienced normal light–dark (L-D) and dark–light (D-L) transitions or transitions that were unexpectedly imposed. We found that expected transitions had a very modest effect on firing rates of both excitatory and inhibitory neurons, even when examined immediately around the time of the transition. Population activity did not change significantly across these transitions; when examined at the level of individual neurons, only a small subset (~15%) of putative excitatory neurons consistently responded and then, only during D-L transitions when animals were awake. Interestingly, randomly timed transitions throughout the L-D cycle elicited more consistent responses across sleep–wake states and at both D-L and L-D transitions, and robust and widespread responses to D-L transitions could be unmasked by exposing animals to prolonged darkness for 60 h. These results suggest that the stability normally observed at expected (circadian) L-D and D-L transitions reflects an active process of stabilization. Finally, although

Significance

The firing dynamics of neurons in primary visual cortex (V1) are poorly understood. Indeed, V1 neurons of freely behaving rats fire at the same mean rate in light and darkness. It is unclear how this stability is maintained and whether it is important for sensory processing. We find that transitions between light and darkness happening at expected times have only modest effects on V1 activity. In contrast, both unexpected transitions and light reexposure after extended darkness robustly increase V1 firing. Finally, pairwise correlations in neuronal spiking are significantly higher during the light when natural vision is occurring. These data show that V1 firing rates are actively stabilized while simultaneously allowing for input-dependent changes in correlations between neurons.

Author contributions: A.T.P., E.I.T., S.M.G., B.J.L., J.G., and G.G.T. designed research; A.T.P., E.I.T., S.M.G., B.J.L., and K.B.H. performed research; K.B.H. contributed new reagents/analytic tools; A.T.P., E.I.T., S.M.G., B.J.L., and Y.W. analyzed data; and A.T.P., Y.W., J.G., and G.G.T. wrote the paper.

Reviewers: C.C., Children's Hospital; and C.M.N., University of Oregon.

The authors declare no conflict of interest.

[1]A.T.P., E.I.T., and S.M.G. contributed equally to this work.

[2]Present address: Department of Biology, Washington University in St. Louis, St. Louis, MO 63130.

[3]Present address: Department of Biology, Stanford University, Stanford, CA 94305.

[4]To whom correspondence may be addressed. Email: turrigiano@brandeis.edu.

Published online July 31, 2019.

mean rates were very similar in light and dark, the pairwise correlations between simultaneously recorded neurons were significantly higher in the light than in the dark, even when controlling for behavioral state. Together, our findings show that firing rates in V1 are actively stabilized as animals navigate dramatic changes in the visual environment. This is in contrast to the correlational structure of V1 activity, which more closely tracks visual drive.

Results

Neurons in V1 maintain remarkably similar mean firing rates during extended periods of light and dark, but how L-D transitions affect firing on more rapid timescales in freely viewing and behaving animals is unclear. Here, we use chronic in vivo electrophysiological recordings from freely behaving rats to closely examine the activity of V1 neurons at D-L and L-D transitions in regular (12/12 h) and manipulated L-D cycles and during unexpected transitions. Using previously established methods (13), we follow individual neurons over time and across multiple light transitions. This approach allows us to analyze the dynamics of neuronal activity at different timescales in response to the appearance or disappearance of natural visual stimuli.

The Appearance or Disappearance of Natural Visual Stimuli Has only a Modest Effect on the Mean Firing Rates of V1 Neurons. The firing rates of V1 neurons recorded in freely behaving young rats in light and dark are very similar when averaged in 12-h periods (13). Here, we combine previously and newly acquired datasets and set out to analyze the activity of V1 neurons around the transition from presence to absence of visual input (L-D) and vice versa (D-L) (Fig. 1*A*). Recorded neurons were classified as regular spiking units (RSUs; $n = 96$) or fast-spiking (FS) cells ($n = 32$) based on waveform shape and according to established criteria (Fig. 1*B*) (16, 19). These populations are mostly composed of excitatory pyramidal neurons (RSU) and inhibitory parvalbumin-containing interneurons (FS) (20, 21).

As rats experience L-D or D-L transitions, most neurons showed little change in firing (Fig. 1*C*). We treated each transition as a separate trial and estimated the firing rate for each cell as the average of the perievent time histogram centered on the transition. We first aimed to compare activity at the population level in different stimulus conditions. To this end, we determined whether the distributions of mean firing rates averaged over 10 min on either side of the L-D and D-L transitions were similar to each other. Cumulative distributions in light and dark were indistinguishable for both RSU and FS cells in all conditions (Fig. 1 *D* and *E*) (2-sample Kolmogorov–Smirnov test; RSU, L-D: $P = 0.88$; D-L: $P = 0.99$; FS, L-D: $P = 0.99$; D-L: $P = 1.0$). Similarly, when we compared the distributions using a Wilcoxon rank sum test, we found no difference between the distributions of mean firing rates before vs. after the transitions (Wilcoxon rank sum test; RSU, L-D: $P = 0.677$; D-L: $P = 0.655$; FS, L-D: $P = 0.905$; D-L: $P = 0.827$).

Next, we took advantage of our ability to follow individual neurons across transitions to examine the data in a paired manner, where the firing rate of each neuron was compared before and after the transition. For each neuron, we computed mean firing rate in the 10 min before and after the transition time and averaged across transitions of the same type to estimate the average effect on individual neuronal firing. This analysis revealed a small but consistent change in mean RSU firing rates across both

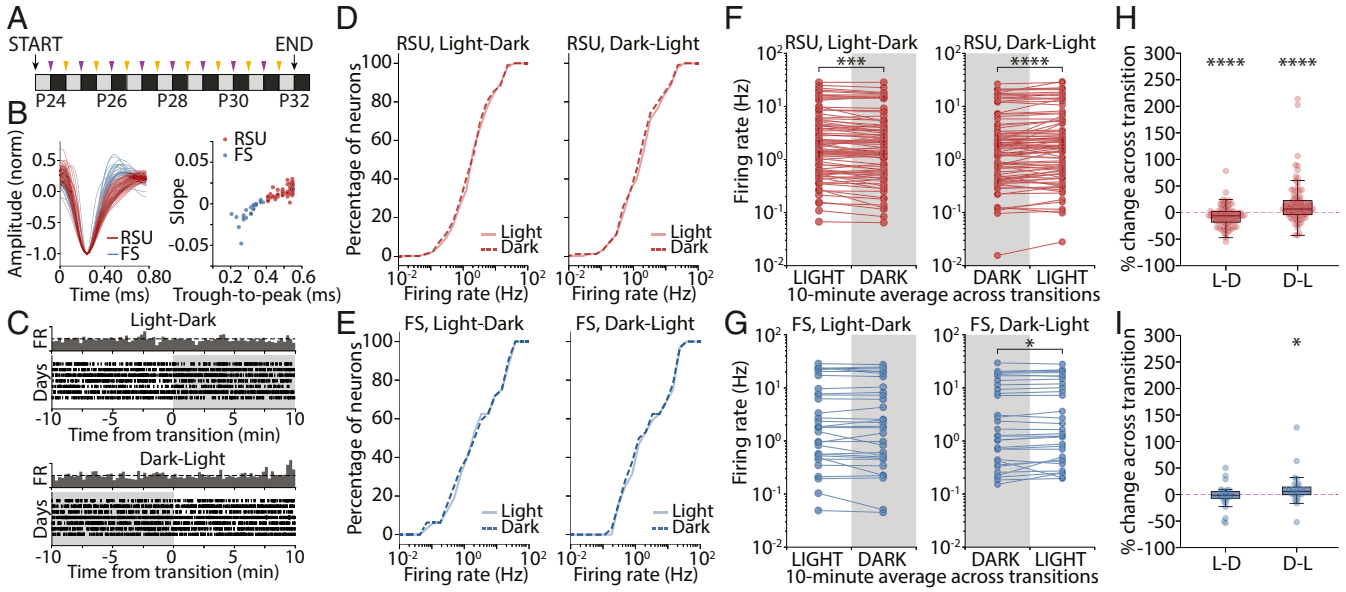

Fig. 1. V1 firing rates are largely stable across circadian L-D and D-L transitions. (*A*) Experimental protocol. Single-unit recordings were obtained from juvenile rats for a continuous 9-d period (P24 to P32). Throughout this period, animals were kept in a regular 12-/12-h L-D cycle and thus, underwent L-D (purple arrows) and D-L (yellow arrows) transitions at regular 12-h intervals. (*B*, *Left*) Average waveform for each continuously recorded unit identified as RSU (red) or FS cell (blue). (*B*, *Right*) Plot of trough-to-peak time vs. waveform slope 0.4 ms after trough reveals the bimodal distribution used to classify recorded units as RSU or FS. (*C*) Example raster plot of spiking activity for a recorded unit across several days, showing 20 min of activity centered on the L-D (*Upper*) and D-L (*Lower*) transitions. Dark bars represent the perievent time histogram obtained by averaging across days. (*D*) Cumulative distributions of RSU firing rates averaged over the 10 min of light (solid lines) or dark (dashed lines) around the transitions for L-D (*Left*) and D-L (*Right*) transitions (L-D, $P = 0.875$; D-L, $P = 0.99$; 2-sample Kolmogorov–Smirnov test). (*E*) As in *D* but for FS units (L-D, $P = 0.99$; D-L, $P = 1.0$; 2-sample Kolmogorov–Smirnov test). (*F*) Mean firing rate for each RSU averaged across all transitions experienced by that neuron in L-D (*Left*) and D-L (*Right*) transitions. Paired data indicate that the average FR is for the same neuron. Distributions were not significantly different (L-D, $P = 0.677$; D-L, $P = 0.655$; Wilcoxon rank sum test), but individual neurons across the whole distribution showed consistent changes at the transitions. ***$P = 0.0002$; ****$P < 0.0001$ (Wilcoxon signed rank test). (*G*) As in *F* but for FS units. Distributions were not different (L-D, $P = 0.905$; D-L, $P = 0.827$; Wilcoxon rank sum test), but individual FS units changed their firing consistently at D-L but not L-D transitions (L-D, $P = 0.318$). *$P = 0.026$ (Wilcoxon signed rank test). (*H*) Percentage of change in firing rate across transition for RSUs (L-D, −7.09 ± 1.99%; D-L, 15.60 ± 4.00%; Wilcoxon signed rank test). ****$P = 0.0001$. (*I*) As in *H* for FS units. Percentage of change in FR was different from 0 in the D-L but not the L-D condition (L-D, −2.75 ± 3.80%, $P = 0.410$; D-L: 9.73 ± 5.12%; Wilcoxon signed rank test). *$P = 0.017$.

L-D and D-L transitions (Fig. 1*F*) (Wilcoxon signed rank test; L-D: $P = 0.0002$; D-L: $P = 0.0001$), while the activity of FS cells only changed significantly at D-L transitions (Fig. 1*G*) (Wilcoxon signed rank test; L-D: $P = 0.318$; D-L: $P = 0.026$). The magnitude of these effects was small: on the order of 7 to 15% for RSUs (Fig. 1 *H* and *I*) (RSU, L-D: $-7.09 \pm 1.99\%$, $P = 0.0001$; D-L: $15.60 \pm 4.00\%$, $P < 0.0001$; FS, L-D: $-2.75 \pm 3.80\%$, $P = 0.410$; D-L: $9.73 \pm 5.12\%$, $P = 0.017$; Wilcoxon signed rank test).

These data show that, surprisingly, dramatic changes in visual input cause very minor changes in V1 firing rates. The distributions of mean rates in the presence and absence of natural visual stimuli are identical in the proximity of transitions. Analysis of many transitions shows that RSU firing rates are consistently affected when the visual environment changes, but this modulation is decidedly modest.

Behavioral State Affects Sensitivity of Firing Rates to Visual Stimuli. As rats were freely behaving throughout, we considered whether their alertness state at the light transitions could affect the activity of V1 neurons. Local field potential (LFP), electromyography (EMG), and video data were collected and used to score animals' behavioral state into either asleep or awake (13). For each animal, 20-min periods centered on the L-D and D-L transitions were considered. Only periods during which the animal remained in the same behavioral state for the entire time were analyzed. For each neuron, we plotted the mean firing rate before the transition against the mean rate after the transition. The activities of neurons proved to be strikingly similar across all transitions regardless of whether the animals were awake or asleep (Fig. 2 *A* and *B*). In either behavioral state, firing rates in light and dark were very strongly correlated, and the slope of the regression line was close to 1 (RSU, wake, L-D: slope = 0.959, $r = 0.966$, $P < 10^{-43}$; D-L: slope = 0.960, $r = 0.991$, $P < 10^{-48}$; FS, wake, L-D: slope = 1.113, $r = 0.964$, $P < 10^{-13}$; D-L: slope = 0.976, $r = 0.990$, $P < 10^{-18}$; RSU, sleep, L-D: slope = 1.147, $r = 0.941$, $P < 10^{-12}$; D-L: slope = 0.990, $r = 0.996$, $P < 10^{-13}$; FS, sleep, L-D: slope = 1.093, $r = 0.987$, $P < 10^{-13}$; D-L: slope = 1.003, $r = 0.996$, $P < 10^{-11}$).

We again looked at the data in paired form by comparing a neuron's average firing rate on either side of an L-D transition. The mean activity of RSUs in V1 changed consistently across transitions when animals were awake (Fig. 2*C*) (L-D: $P = 0.0001$; D-L: $P = 0.0457$; Wilcoxon signed rank test) but not when they were asleep (Fig. 2*D*) (L-D: $P = 0.656$; D-L: $P = 0.925$; Wilcoxon signed rank test). We observed a similar pattern in FS cells, although the data in the wake condition were not significant for L-D transitions (Fig. 2 *E* and *F*) (wake, L-D: $P = 0.689$; D-L: $P = 0.039$; sleep, L-D: 0.557; D-L: $P = 0.638$; Wilcoxon signed rank test). Once again, these effects were of small magnitude (7 to 12%). Thus, V1 neurons do not respond to expected (circadian) changes in the visual environment when animals are asleep and respond only modestly when animals are awake.

A Subpopulation of RSUs Is Consistently Responsive to D-L Transitions. While we only detected small changes at the population level (and no change in the population distribution), we occasionally observed neurons with activity that appeared to be consistently modulated by visual stimuli. The majority of neurons showed no spiking modulation across multiple transitions (Fig. 3*A*), but a subset of neurons showed higher activity on 1 side of the transition (Fig. 3*B*). Occasionally, neurons responded to both L-D and D-L transitions (Fig. 3*B*), but more often, neurons were only responsive to one or the other. To quantify these observations, we treated each transition independently for each neuron, averaged firing rates for 10 min before and after lights on/off, and identified neurons that changed their firing rate consistently across transitions using a paired *t* test.

Because neuronal firing rates are variable, we presumed that some of these apparent responses were spurious. To estimate the false positive rate, we performed a bootstrap analysis using random time points as dummy "transitions." We chose 9 transition points 24 h apart from each other (to match circadian transitions) and analyzed mean firing rates for each neuron as above but using these dummy transition points. This process was repeated 100 times to arrive at an estimate of the mean and 95% confidence interval (95% CI) for the percentage of responsive

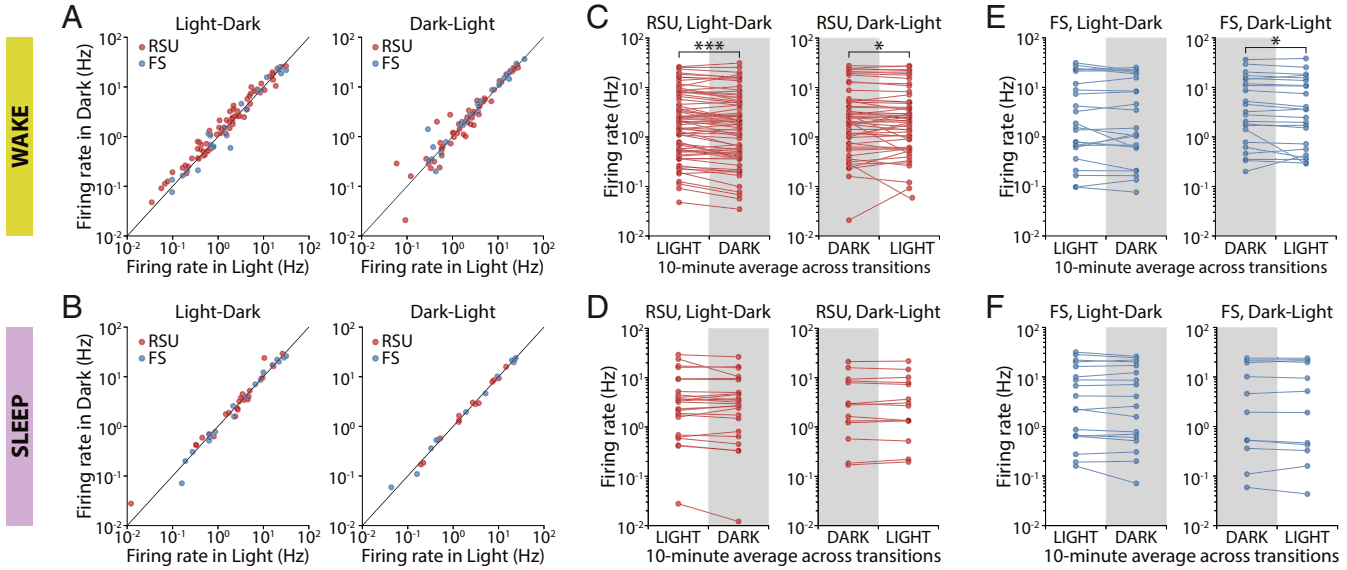

Fig. 2. L-D transitions modestly modulate the firing of V1 neurons during wake but not sleep. (*A*) Comparison of mean firing rates in 10-min averages around the transitions in L-D and D-L transitions when the animal was awake for the whole 20 min. Activity in light and dark was strongly correlated for both transition types. (*B*) As in *A* but for transitions during which animals were asleep for the 20-min period around the transition. Firing rates in light and dark during sleep were also strongly correlated. (*C*) Mean firing rate of individual RSUs calculated in 10-min averages around luminance transitions and averaged across all transitions during which animals were awake. Neuronal activity changed consistently at the transitions (***$P = 0.0001$; *$P = 0.0457$; Wilcoxon signed rank test). (*D*) As in *C* but for transitions during which animals were asleep. No significant change was observed (L-D, $P = 0.656$; D-L, $P = 0.925$; Wilcoxon signed rank test). (*E*) As in *C* for FS units. Cells' activity only changed significantly at D-L transitions (L-D, $P = 0.689$; D-L, *$P = 0.039$; Wilcoxon signed rank test). (*F*) As in *D* for FS cells. No significant change was observed (L-D, $P = 0.557$; D-L, $P = 0.638$; Wilcoxon signed rank test).

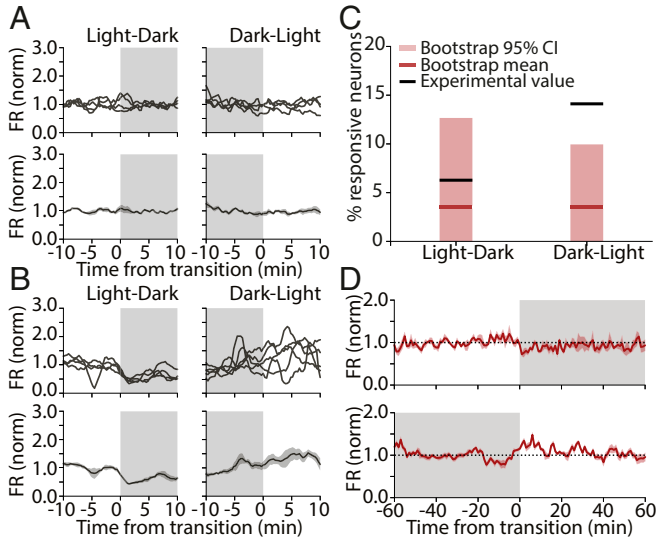

Fig. 3. A subset of RSUs consistently increases their firing rate in response to expected D-L transitions. (*A*) Example of an RSU unresponsive to light transitions (*Left*, L-D; *Right*, D-L). (*Upper*) Binned firing rate for each transition; (*Lower*) average across transitions. (*B*) Example RSU that responds consistently to light transitions. (*C*) Percentage of RSUs found to be responsive to L-D (*Left*) and D-L (*Right*) transitions and bootstrap control. Black lines show experimental values (actual percentages of responsive neurons); red lines show bootstrap means. Light red bars show the extent of the bootstrap 95% CI (L-D, actual value: 6.25%, bootstrap mean: 3.55%; 95% CI: 0 to 12.62%; D-L, actual value: 14.06%; bootstrap mean: 3.09%; 95% CI: 0 to 9.91%; $n = 64$). (*D*) Mean firing rate averaged across transitions for all D-L–responsive RSUs calculated for 2 h around each transition for L-D (*Upper*) and D-L (*Lower*) transitions. The transient nature of the firing-rate response is visible in *Lower*.

cells (mean [95% CI], RSU, L-D: 3.55% [0 to 12.62%]; D-L: 3.09% [0 to 9.91%]; $n = 64$).

The proportion of cells that we found to be transition responsive was within the range expected by chance for all conditions except for RSUs in D-L transitions (Fig. 3*C*). We found that 14% of RSUs in our experimental condition had significantly changing firing rates from dark to light, well outside the range expected by chance (95% CI for this group: 0 to 9.91%). In addition, most of these neurons (88.9%) showed an increase in firing rate at the onset of light, while in the bootstrap control, neurons were found to have an equal probability of increasing or decreasing their activity at a given transition point (51.8% of neurons increasing).

Finally, we examined the temporal dynamics of firing-rate changes for the subset of RSUs that were consistently responsive to D-L transitions. We plotted the mean activity within 1 h of the transition, across all transitions, and across neurons for this subpopulation (Fig. 3*D*). On average, the change in firing rate was short lived (on the order of ∼10 min) and of moderate size (∼25% increase). This analysis shows that a small subset of excitatory pyramidal neurons in V1 consistently modulates their activity in response to the expected appearance of visual input after a circadian 12-h period of darkness. This change is transient, with firing rates returning to pretransition levels within minutes.

Light Transitions Have No Effect on Average Interspike Intervals over Short Timescales. Our analysis so far shows that, on a timescale of tens of minutes, few V1 neurons show significant firing-rate modulation to the appearance or disappearance of natural visual stimuli. One possible explanation for this apparent lack of responsiveness is that these dramatic sensory changes trigger a rapid adaptation mechanism that quickly restores average V1 activity back to baseline. Such adaptation mechanisms within V1 have been well described and can operate on a timescale of hundreds of milliseconds to many minutes (22–24). To address this possibility, we examined neuronal firing in 1-, 10-, and 30-s intervals around L-D and D-L transitions for RSUs in our dataset. Spiking in these short time windows was sparse and variable across days (Fig. 4 *A* and *B*). We averaged the mean interspike interval (ISI) across days for each cell and compared averages in the 10 s before and after transitions. To ensure that we were not missing effects on even shorter timeframes, we also computed the mean ISI in 1-s windows around the transitions. For both the 1- and 10-s cases, we found no statistically significant effect (Fig. 4 *C*, 1 s, L-D: $P = 0.27$; D-L: $P = 0.36$; and *D*, 10 s, L-D: $P = 0.97$; D-L: $P = 0.31$; Wilcoxon signed rank test). Similar results were obtained when this analysis was carried out with 5- and 30-s intervals. This indicates that the stability of firing across transitions is not due to a short-term adaptation process that rapidly restores firing to baseline.

Pairwise Correlations in V1 Are Significantly Higher in Light than in the Dark. To investigate whether higher-order network properties are modified by the presence or absence of natural visual stimuli, we examined the structure of pairwise correlations in light and in dark (Fig. 5) ($n = 5$ animals). Plotting the correlation matrices of 1 animal at postnatal day 27 (P27) revealed that these correlations were higher in the light (calculated over the 12-h period at P27) than in the dark (calculated over the 12-h period at P27.5) (Fig. 5*A*). We then plotted the average correlation computed continuously over 4 d (normalized to the average correlation of each animal at P26 in light) (Fig. 5*B*). The normalized pairwise correlation showed a pronounced oscillation across light and dark periods and was consistently higher in the light. To assess the degree to which correlation of individual pairs changed, we compared the correlation of 922 pairs in light vs. dark computed for spike counts with bin sizes of 5 or 100 ms, respectively. We found that correlations in light were higher than in the dark for both bin sizes (Fig. 5 *C*, *Left*, 5 ms: $P < 10^{-70}$ and *Right*, 100 ms: $P < 10^{-125}$; Wilcoxon signed rank test). To ensure that the observed difference of correlations between light and dark was not caused by disproportionate time spent in wake or sleep, we

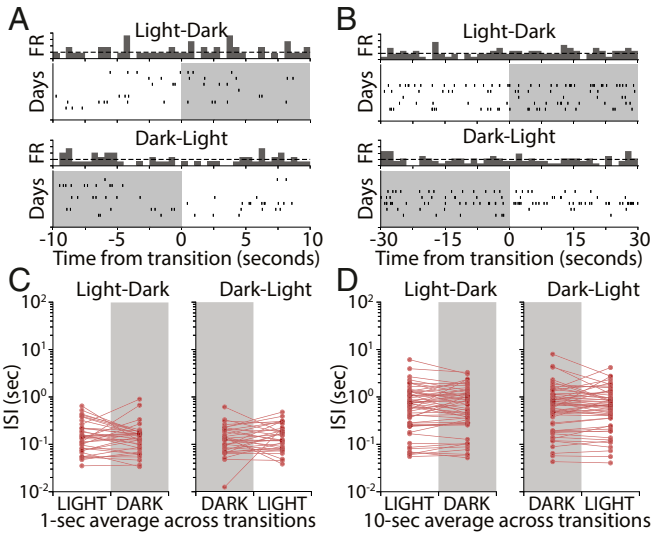

Fig. 4. L-D and D-L transitions have no effect on V1 firing rates over short timescales. (*A*) Raster plot showing activity of an example RSU in a 10-s interval around L-D and D-L transitions. Vertical ticks represent spikes, and rows represent transitions happening on different recording days. (*B*) A second example RSU showing a 30-s interval around transitions. (*C*) Mean ISIs for all recorded cells obtained by averaging ISIs in 1-s bins around L-D and D-L transitions for different days. Each dot represents the mean for 1 cell obtained by averaging across days. No significant change was observed (L-D, $P = 0.27$; D-L, $P = 0.36$; Wilcoxon signed rank test). (*D*) As in *C* but for 10-s averages. No significant change was observed (L-D, $P = 0.97$; D-L, $P = 0.31$; Wilcoxon signed rank test).

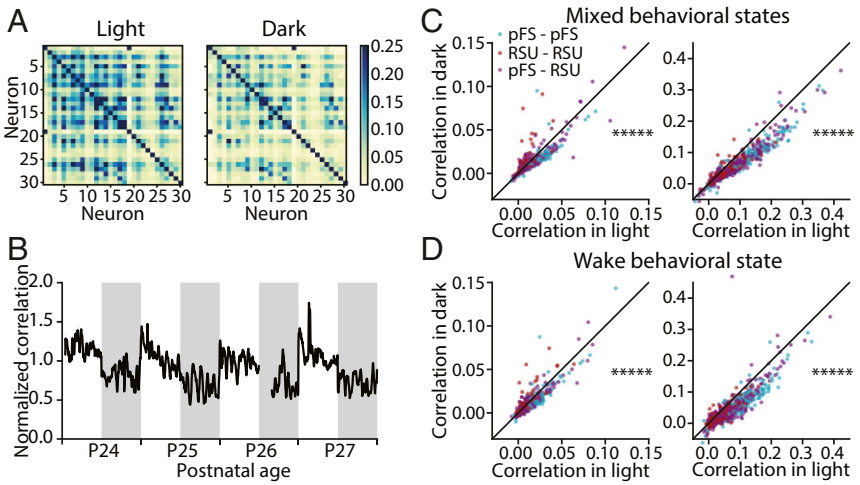

Fig. 5. Pairwise correlations in V1 are higher during light than during dark. (*A*) Example pairwise correlation structure of 30 neurons from a single animal during light (*Left*; calculated over the 12-h period at P27) and during dark (*Right*; calculated over the 12-h period at P27.5). (*B*) The average correlation of 922 pairs from 5 animals over 4 d normalized to the average correlation of each animal relative to P26 in light. The gap in the data at P26 corresponds to the time that animals were anesthetized for monocular deprivation, which was excluded from analysis. (*C*) Comparison of the average correlation of 922 pairs during light and during dark with bin size 5 ms (*Left*) and bin size 100 ms (*Right*). (*Left*) *****$P < 10^{-70}$ (Wilcoxon signed rank test). (*Right*) *****$P < 10^{-125}$ (Wilcoxon signed rank test). (*D*) Comparison of average correlation of 922 pairs in wake during light and during dark with bin size 5 ms (*Left*) and bin size 100 ms (*Right*). (*Left*) *****$P < 10^{-55}$ (Wilcoxon signed rank test). (*Right*) *****$P < 10^{-110}$ (Wilcoxon signed rank test). pFS, putative fast-spiking neurons.

restricted the analysis to periods of wake and again computed the average correlation. Consistent with our previous analysis, correlations in wake during light were significantly greater than in wake during dark (Fig. 5 *D*, *Left*, 5 ms: $P < 10^{-55}$ and *Right*, 100 ms: $P < 10^{-110}$; Wilcoxon signed rank test). These results indicate that the presence of natural visual stimuli increases pairwise correlations in V1.

Noncircadian, Unexpected L-D Transitions Are More Likely to Perturb V1 Firing Rates. All of our data so far suggest that dramatic changes in visual input at circadian L-D transitions have very subtle effects on V1 firing. We wondered if this might be due to circadian entrainment (i.e., that when L-D and D-L transitions happen at regular times, they are expected, and the response of neurons to otherwise salient stimuli is attenuated). To test this, we examined neuronal responses to stimulus transitions occurring at random points in the circadian cycle.

We recorded single-unit activity in V1 in a different subset of animals while turning the lights off (or on) for 10 min during the light (or dark) cycle (Fig. 6*A*) ($n = 6$ animals). We then calculated the number of neurons that consistently and significantly changed their firing at these unexpected transitions and again, used a bootstrap analysis to calculate the false positive rate. In marked contrast to expected transitions (Fig. 3*D*), we found that both L-D and D-L unexpected transitions caused a subset of RSUs to consistently modulate their spiking (Fig. 6 *B* and *C*). This effect was seen regardless of behavioral state (significantly changing RSUs, sleep, L-D: 21.9%, $n = 64$; D-L: 13.4%, $n = 67$; wake, L-D: 17.6%, $n = 91$; D-L: 12.7%, $n = 55$), and the proportion of significantly changing neurons was higher than expected by chance in most conditions (bootstrap mean [95% CI]; RSU, sleep, L-D: 4.42% [0 to 8.95%]; D-L: 4.31% [0 to 9.38%]; RSU, wake, L-D: 4.22% [0 to 8.79%]; D-L: 4.33% [0 to 9.09%]). These results show that more neurons respond consistently to L-D and D-L transitions when these do not line up with the circadian cycle that the animals are entrained on. However, even during these unexpected transitions, only a minority (12 to 20%) of neurons consistently changed their firing rate in response to the appearance or disappearance of natural visual stimuli.

To further examine the nature of these responses, we averaged and plotted the activity of the subpopulation of responsive units for each combination of behavioral state and transition type (Fig. 6 *D* and *E*). In the wake state, there was a net decrease in firing during L-D transitions and vice versa for D-L (Fig. 6*E*), whereas there was little net change during sleep (Fig. 6*D*). This is likely due to averaging over changes in opposite directions during sleep, as 4 of 14 cells (29%) increased their FR in L-D transitions and 5 of 9 cells (55%) increased their FR in D-L transitions. However, even in wake, these firing-rate changes were on the order of 10 to 25%, indicating that, even under the most permissive conditions, firing is only subtly modulated by brief L-D transitions.

Prolonged Dark Exposure Enhances the Responsiveness of V1 Neurons to Natural Visual Input. Our data show that reexposure to light after 12 h of darkness has only modest effects on V1 firing; in contrast, reexposing animals to light after a period of prolonged darkness is a standard paradigm for increasing activity-dependent gene expression in V1 (refs. 25–27; reviewed in ref. 28). We, therefore, wondered whether prolonged dark exposure might unmask robust responses to the sudden onset of visual stimuli within V1.

We began by using expression of the immediate early gene *c-fos*, which is driven by enhanced calcium influx during elevated activity (refs. 29 and 30; reviewed in ref. 31). After prolonged darkness, brief light exposure induces widespread *c-fos* expression in V1 of cats and rodents (25, 32–34). To replicate this, we placed P26 rats in the dark for 60 h (12 h + 2 d) and then, exposed them to light for 1 h before immunostaining for the c-fos protein (light exposed, $n = 28$ slices, 5 animals). We used age-matched animals either exposed to 1 h of light after a regular 12-/12-h cycle (regular control, $n = 22$ slices, 4 animals) or kept in the dark for 60 h but killed before lights on (dark control, $n = 23$ slices, 4 animals) as controls (Fig. 7 *A* and *B*). Animals in the light exposure condition showed an elevated percentage of c-fos–positive cells (Fig. 7 *C*, *Upper*) (regular control: 11.4 ± 1.6%; dark control: 6.1 ± 0.8%; light exposed: 16.8 ± 1.7%; light exposed vs. regular control $P = 0.032$; light exposed vs. dark control $P = 0.001$; 1-way ANOVA with Tukey post hoc test) as well as increased total staining intensity (Fig. 7 *C*, *Lower*) (normalized to regular control; regular control: 1.00 ± 0.06; dark control: 0.79 ± 0.05; light exposed: 1.31 ± 0.09; light exposed vs. regular control $P = 0.011$; light exposed vs. dark control $P = 0.001$; 1-way ANOVA with Tukey post hoc test). These data confirm that a 60-h period of prolonged darkness is sufficient to up-regulate c-fos in rodent V1 on light reexposure.

Next, we asked whether elevated c-fos expression was correlated with increased firing. We used the same paradigm as above but recorded continuously from V1 during the baseline, dark exposure, and light reexposure periods ($n = 4$ animals). On light reexposure, both RSUs and FS cells showed a substantial transient increase in firing rate at the time of lights on (Fig. 7*D*) (RSU: $n = 32$; FS: $n = 12$). We compared average firing rates 10 min before and after the transition for each cell. Both FS and RSU populations showed a significant increase in firing rate after light reexposure (Fig. 7 *F* and *G*) (RSU: $P < 10^{-5}$; FS: $P = 0.034$; Wilcoxon signed rank test). The percentage change in firing rate across the transition was also significantly different from 0 (Fig. 7*E*) (all cells: 87.1 ± 13.5%, $P < 10^{-7}$; RSU: 80.7 ± 14.9%, $P < 10^{-5}$; FS: 104.3 ± 29.8%, $P = 0.005$; 1-sample *t* test),

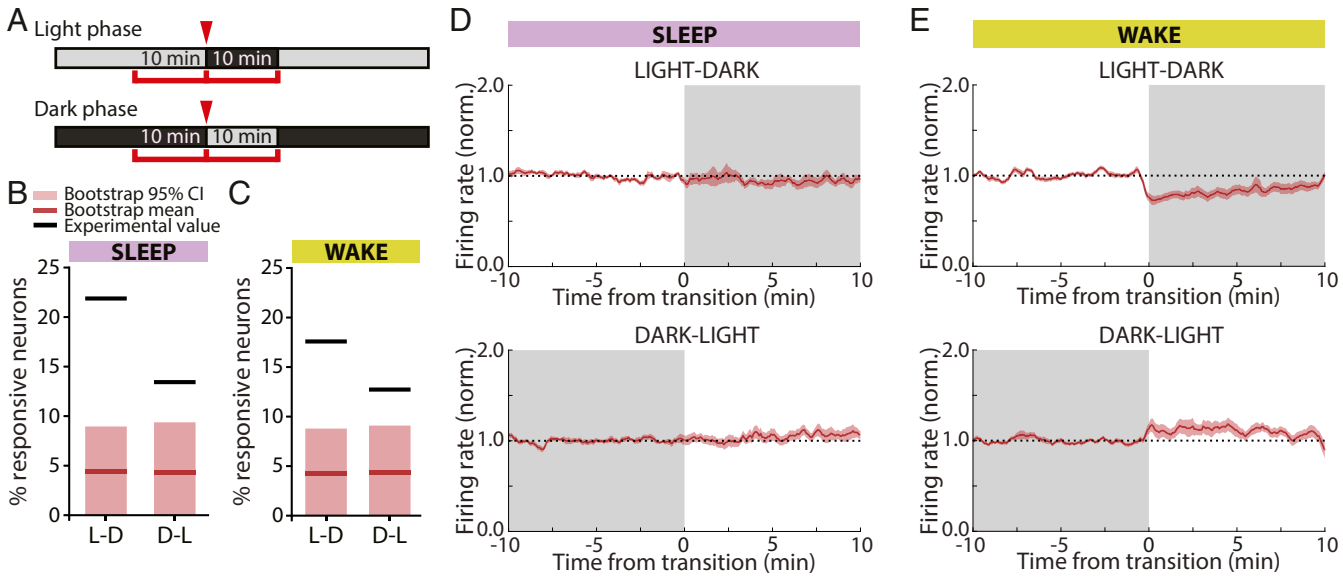

Fig. 6. Randomly timed L-D and D-L transitions induce consistent firing-rate changes in RSUs. (*A*) Experimental design. Animals were exposed to 10-min periods of darkness during the light phase and 10-min periods of light during the dark phase at random points throughout the L-D cycle. Mean firing rates were calculated in 10-min intervals around the transition. (*B*) Percentage of RSUs that were responsive to L-D and D-L transitions when transitions happened in epochs of sleep. Black lines shows actual experimental values; red lines show bootstrap means. Light red bars cover the bootstrap 95% CIs (sleep, L-D: 21.9%, bootstrap mean [95% CI]: 4.42% [0 to 8.95%], $n = 64$; D-L: 13.4%, bootstrap mean [95% CI]: 4.31% [0 to 9.38%], $n = 67$). (*C*) As in *B* but for transitions happening while animals were awake (wake, L-D: 17.6%, bootstrap mean [95% CI]: 4.22% [0 to 8.79%], $n = 91$; D-L: 12.7%, bootstrap mean [95% CI]: 4.33% [0 to 9.09%], $n = 55$). (*D*) Mean firing rates of units that consistently responded to visual input changes in sleep averaged across cells and transitions for L-D (*Upper*) and D-L (*Lower*) transitions. Ten minutes on either side of the transition are shown. (*E*) As in *D* for units responsive during wake transitions.

and the majority of neurons increased their activity at lights on (RSU: 31 of 32 neurons; FS: 10 of 12 neurons).

One possible cause of enhanced responsiveness at salient unexpected transitions (i.e., those happening after prolonged darkness or at noncircadian times) (Fig. 6) is that responses are normally suppressed when transitions are anticipated. If so, we would expect to see an opposite effect on firing when an expected transition does not occur. To look for such an effect, we examined firing rates during prolonged dark exposure at the times when expected (circadian) L-D transitions did not occur (Fig. 8 *A* and *B*, "missing" transitions). We found a nonsignificant trend toward reduced firing across the population at missing D-L transitions (Fig. 8 *A*, *Lower Right*) and a small but significant increase in firing at missing L-D transitions (Fig. 8 *B*, *Lower Right*). Because we had only 2 repetitions of each transition, we could not quantify the fraction of neurons that responded consistently to expected transitions that did not occur.

Finally, it has been reported that prolonged dark exposure increases firing rates in rodent V1 (35), suggesting that enhanced responsiveness to light reexposure might arise from increased excitability of V1 circuitry. To examine this, we asked how prolonged dark exposure affected RSU firing rates in freely behaving animals before light reexposure. When we compared the distribution of RSU firing rates during the first and last 12 h of the 60-h-long period of prolonged darkness, rather than an increase, we found a small but significant decrease in firing rates (Fig. 8*C*) (mean ± SEM; first 12 h: 4.00 ± 0.97 Hz, last 12 h: 2.27 ± 0.57 Hz; median; first 12 h: 1.18 Hz; last 12 h: 0.85 Hz; $P = 0.044$; Wilcoxon rank sum test). Thus, the enhanced responsiveness to restoration of natural visual stimuli is unlikely to be due to a simple global increase in circuit excitability.

In summary, these data indicate that prolonged dark exposure disrupts the normal stability of V1 firing across D-L transitions and suggest that the maintenance of this stability is dependent on visual experience.

Discussion

How internal and external factors influence the long-term dynamics of neuronal firing in V1 is poorly understood. Here, we recorded from ensembles of single units over a period of several days in freely viewing and behaving animals and found that firing rates of both excitatory and inhibitory V1 neurons were remarkably stable even when sensory input changed abruptly and dramatically. During expected circadian L-D transitions, very few V1 neurons significantly changed their firing. A larger subset of V1 neurons was consistently responsive to unexpected L-D transitions, and disruption of the regular L-D cycle with 2 d of complete darkness induced a widespread and robust increase in V1 firing on subsequent reintroduction of visual input. These data show that most V1 neurons fire at similar rates in the presence or absence of natural visual stimuli and that significant changes in mean activity arise only in response to unexpected changes in the visual environment. While mean firing rates were not different in light and dark, pairwise correlations were significantly stronger in the light in the presence of natural visual stimuli, even when controlling for behavioral state. Taken together, our findings are consistent with a process of rapid and active stabilization of firing rates during expected changes in visual input and demonstrate that firing rates in V1 are remarkably stable at both short and long timescales.

The near absence of firing-rate modulation in response to the appearance (or disappearance) of natural visual stimuli may seem surprising, as there is a rich literature supporting the idea that V1 neurons respond to optimal stimuli by increasing their spiking (36–44). Many of these studies used anesthetized preparations, making comparisons with our results difficult, but our data are consistent with previous reports of small differences in overall activity between natural vision and complete darkness in awake animals (8) and sparse modulation of spiking in response to natural scene viewing (12, 45–47). In general, our data support the view that mean firing rates in V1 can be stabilized over both long (13) and short timescales without interfering with visual coding, which may arise through very sparse modulation of spiking and/or higher-order population dynamics (46, 48, 49).

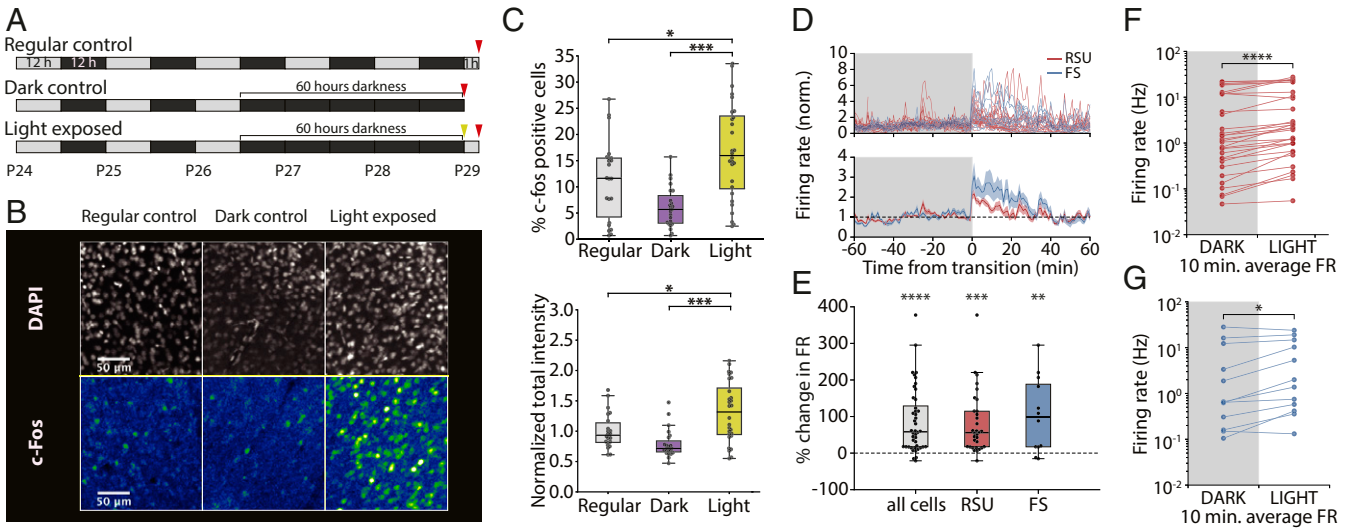

Fig. 7. Light reexposure after prolonged darkness results in increased c-fos expression and increased neuronal firing in V1. (*A*) Experimental protocol. Animals were exposed to a regular 12-/12-h L-D cycle and killed 1 h after lights on at P29 (regular control, $n = 22$ slices, 4 animals), exposed to darkness for 60 h starting at P26 and killed before lights on (dark control, $n = 23$ slices, 4 animals), or exposed to 60 h of darkness starting at P26 and killed 1 h after light reexposure (light exposed, $n = 28$ slices, 5 animals). (*B*) Representative images showing DAPI (*Upper*) and c-fos (*Lower*) immunostaining for regular control (*Left*), dark control (*Center*), and light-exposed (*Right*) animals. (*C*, *Upper*) Percentage of c-fos–positive cells in all 3 groups (regular control: 11.4 ± 1.6%; dark control: 6.1 ± 0.8%; light exposed: 16.8 ± 1.7%). $^{*}P = 0.032$ (1-way ANOVA with Tukey post hoc test); $^{***}P = 0.001$ (1-way ANOVA with Tukey post hoc test). (*C*, *Lower*) Total colocalized DAPI and c-fos staining intensity normalized to average of regular control group (regular control: 1.00 ± 0.06; dark control: 0.79 ± 0.05; light exposed: 1.31 ± 0.09). $^{*}P = 0.011$ (1-way ANOVA with Tukey post hoc test); $^{***}P = 0.001$ (1-way ANOVA with Tukey post hoc test). (*D*) Time course of RSU and FS spiking in a 2-h period around the time of light reexposure. Individual unit traces (*Upper*) and average across cells (*Lower*) show marked increase in firing at the time of lights on. (*E*) Percentage of change in firing rate between the 10 min before and the 10 min immediately after light reexposure (all cells, 87.1 ± 13.5%, $n = 44$; RSU, 80.7 ± 14.9%, $n = 32$; FS, 104.3 ± 29.8%, $n = 12$, 1-sample t test). $^{**}P = 0.005$; $^{***}P < 10^{-5}$; $^{****}P < 10^{-7}$. (*F*) Mean firing rate in the 10 min before and after the transition for each recorded RSU. $^{****}P < 10^{-5}$ (Wilcoxon signed rank test). (*G*) As in *F* for recorded FS cells. $^{*}P = 0.034$ (Wilcoxon signed rank test).

Despite the lack of robust changes in firing rates across the population at D-L transitions, we did observe a small subset of neurons that transiently increased their firing specifically at the appearance of visual input (Fig. 3). Interestingly, many layer 4 (L4) neurons (which account for 34% of our dataset) did not show this kind of transient response at D-L transitions. The subset of responsive neurons included cells from L4 but also, all other layers of V1. Since this occurred in freely viewing animals, it is unlikely that these neurons were responding to the same specific visual stimuli on successive days. A more parsimonious explanation is that these neurons are activated by luminance changes at most D-L transitions. One possible source of drive to these neurons is from intrinsically photosensitive retinal ganglion cells (ipRGCs), which are known to exhibit prolonged changes in firing on changes in luminance (50–52). Some classes of ipRGCs have been shown to project to the dorsolateral geniculate nucleus (dLGN) of mice, where they modulate the firing of ∼20 to 30% of dLGN neurons (53–55) and thus, can influence activity in V1 (53). The firing of V1 neurons activated by L-D transitions adapted over the first several minutes, but whether all ipRGC firing adapts over a similar timescale is not known (53–55). There is evidence that the ipRGCs of the M1 class can produce persistent responses, resulting in temporal integration over several minutes (56). It is at least plausible that the activity of these cells is contributing to the coding of light levels in V1. Unfortunately, it is difficult to directly test the role of ipRGCs in V1 responses in rats, as transgenic animals that would allow the selective activation of ipRGCs without activating rods or cones (as for mouse) (54, 55, 57) are not currently available. While it is possible that this small subset of responsive neurons represents sparse coding for the transition event, it is equally possible that this is a simple reflection of upstream changes in activity and that V1 does not explicitly code for sharp light transitions.

Interestingly, we detected a greater proportion of transition-responsive cells when light transitions happened randomly throughout the L-D cycle, including a population of neurons that transiently responded to noncircadian L-D transitions by decreasing their firing rate (Fig. 6). Thus, unexpected changes in visual drive unmask robust and bidirectional changes in firing in a small subset (15 to 20%) of V1 neurons. We observed a similar effect when expected L-D transitions did not occur, which unmasked an increase in firing. There are several potential explanations for this effect. It is possible that the responsive neurons are specialized to represent this "unexpectedness" as an error signal, such as has been proposed in some models of predictive coding (58, 59). Alternatively, it could be the result of modulation by other brain areas that encode the surprise signal, akin to that seen in response to attention or reward cues (60, 61) or during modulation of V1 by locomotion (62).

We were able to disrupt the normal conservation of firing rates across D-L transitions even more dramatically by using a prolonged dark-exposure paradigm, which induced a network-wide enhancement of firing on light reexposure. This paradigm is thought to induce metaplastic changes within V1 that increase α-amino-3-hydroxy-5-methyl-4-isoxazolepropionic acid (AMPA) quantal amplitude onto L2/3 pyramidal neurons (35, 63, 64), but the impact of these changes on overall V1 function and excitation/inhibition balance is unclear. A previous study in anesthetized animals found that several days of dark exposure increased firing rates in V1, raising the possibility that prolonged dark exposure increases overall V1 excitability (35); however, here we found a small but significant reduction in mean firing rate across the population in freely behaving animals, suggesting that circuit excitability is, if anything, reduced by 60 h of dark exposure. Interestingly, this change in firing rate (FR) does not seem to trigger a homeostatic compensation in the opposite direction. This could be because a slow and gradual shift in neuronal FR set points occurs during darkness, or perhaps, we are simply reintroducing light before homeostatic changes have a chance to influence FRs. Although the circuit mechanism by which dark exposure unmasks

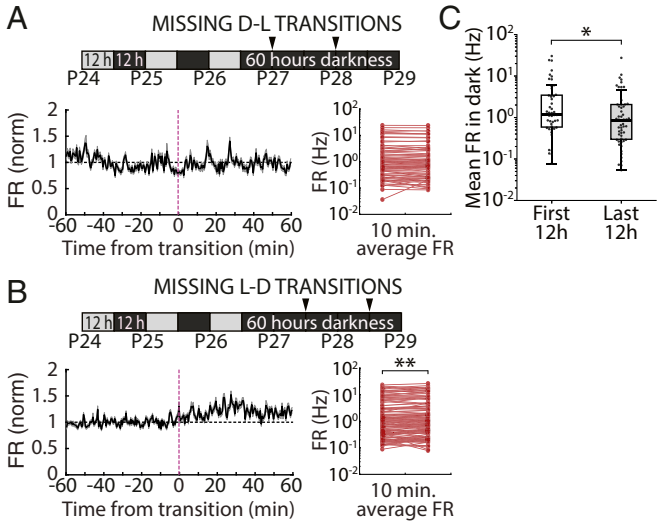

Fig. 8. Firing-rate dynamics in V1 during prolonged darkness. (*A*) Mean firingrate dynamics of RSUs recorded during 60 h of continuous dark exposure at expected D-L transitions that did not occur (missing transitions). (*Lower Left*) Firing rate in a 2-h period around the missing transition averaged across all neurons and both transitions. (*Lower Right*) Average FR for all neurons calculated in 10-min bins before and after the transition, showing no change in activity when lights did not come on at the expected D-L transitions (4.56 ± 5.94%, $P = 0.162$; Wilcoxon signed rank test). (*B*) As in *A* but for L-D transitions. We found a significant increase in FR when L-D transitions were expected but did not occur (10.70 ± 2.75%, $^{**}P = 0.0045$; Wilcoxon signed rank test). (*C*) Mean firing rate for all recorded RSUs averaged across the first 12-h period within the 60 h of darkness (first 12 h, mean ± SEM: 4.00 ± 0.97 Hz, median: 1.18 Hz, $n = 47$) and the last 12-h period of darkness before light reexposure (last 12 h, mean ± SEM: 2.27 ± 0.57 Hz, median: 0.85 Hz, $n = 55$). $^{*}P = 0.044$ (Wilcoxon rank sum test).

robust responses to D-L transitions is unclear, these experiments suggest that normal visual experience is necessary to maintain the ability of V1 circuits to stabilize their firing across these transitions.

In contrast to our observations on the stability of firing rates, we found that pairwise correlations in visual cortex were markedly higher in the light phase than in the dark phase (Fig. 5). This is consistent with previous reports that ongoing spontaneous activity in the dark is less correlated than activity elicited by natural scene stimuli (8, 65). Correlations are dependent on the degree of synchrony within neuronal circuits (66, 67) and are higher during anesthesia (68), raising the possibility that this is a simple reflection of time spent in different behavioral states during the light and dark phase. However, we observed the same increased correlation in light when only analyzing periods when animals were awake, ruling out this possibility. Thus, we conclude that, in freely behaving and viewing animals, sensory input can shift visual cortical circuits to more correlated dynamical states, even in a condition of low synchrony when animals are awake. It should be noted that these correlations may simply reflect the timing of shared visual input to neurons with similar tuning and thus, might not provide additional information above that carried by the timing of individual neuronal responses.

Our results add to a growing body of work suggesting that ongoing activity in mammalian V1 plays an important role in modulating sensory responses as well as in integrating other sensory, motor, and motivational signals (5, 8, 10, 11, 48, 58, 59, 62, 69–75). Our results also show that firing rates of most V1 neurons are remarkably stable over both long and short timescales and in the presence and absence of visual information, suggesting that most visual information during natural viewing is not encoded by changes in firing rates. Instead, our data suggest that perturbations in firing primarily occur during unexpected changes in visual input, indicating an effect of entrainment/expectation and the existence of an active mechanism for stabilization of activity. This may be of particular importance given the observation that pairwise correlations are increased when animals are exposed to visual input, as global fluctuations in firing rate can strongly affect the strength of correlations between pairs of neurons (66). Thus, it is possible that stable firing rates enable changes in correlations to reflect differences in sensory input and hence, to promote effective sensory processing.

Methods

All surgical and experimental procedures were approved by the Animal Care and Use Committee of Brandeis University and complied with the guidelines of the NIH.

Surgery and In Vivo Electrophysiology Experiments. The data analyzed in this study were collected in previous electrophysiological experiments (13; $n = 7$ rats) as well as from a new set of animals ($n = 14$ rats; $n = 21$ rats total). All surgical procedures were as described previously (16). Briefly, Long–Evans rats of either sex were bilaterally implanted with custom 16-channel, 33-μm tungsten microelectrode arrays (Tucker–Davis Technologies) into monocular primary visual cortex (V1m) on P21. Location was confirmed post hoc via histological reconstruction. Two EMG wires were implanted deep in the nuchal muscle. Animals were allowed to recover for 2 full days postsurgery in transparent plastic cages with ad libitum access to food and water. Recording began on the third day after surgery. The recording chamber (a 12- × 12-inch Plexiglas cage with walls lined with high contrast square wave gratings with spatial frequency of 0.3 to 1 cycles/cm) was lined with 1.5 inches of bedding and housed 2 rats. Animals had ad libitum food and water and were separated by a clear plastic divider with 1-inch holes to allow for tactile and olfactory interaction while preventing jostling of headcaps and arrays. Electrodes were connected to commutators (TDT) to allow animals to freely behave throughout the recordings. Novel toys were introduced every 24 h to promote activity and exploration and provide additional visual stimulation. Lighting and temperature were kept constant (L-D 12:12, lights on at 7:30 AM, 21 °C, humidity 25 to 55%). Light levels during light and dark were obtained by measuring irradiance at the cage floor using an optical energy meter (ThorLabs PM100D). Irradiance values were 48.0 μW/m^2 (light) and less than 0.0001 μW/m^2 (dark) for incident light with a wavelength of 510 nm. Data were collected continuously for 9 to 11 d (200 to 240 h). Some animals ($n = 11$ rats) underwent a lid suture and/or eye reopening procedure on the third day of recording; in this study, we only analyzed data collected from the control hemisphere ipsilateral to the manipulated eye. For dark exposure experiments, animals were kept in the dark starting on days 4 and 5 of the recording (i.e., starting at the time of lights off on day 3 from P26 to P28). Lights came on at the regular time (7:30 AM) on day 6 (P29).

Electrophysiological Recordings. In vivo electrophysiological recordings were performed as previously described (13). Briefly, data were acquired at 25 kHz, digitized, and streamed to disk for offline processing using a Tucker–Davis Technologies Neurophysiology Workstation and Data Streamer. Spike extraction and sorting were performed using custom MATLAB code. Spikes were detected as threshold crossings (–4 SD from mean signal) and resampled at 3 times the original rate. Each wire's waveforms were then subjected to principal component analysis, and the first 4 principal components were used for clustering using KlustaKwik (76). Clusters were merged or trimmed as described previously (13). Spike sorting was done using custom MATLAB code relying on a random forest classifier trained on a manually scored dataset of 1,200 clusters. For each cluster identified from the output of KlustaKwik, we extracted a set of 19 features, including ISI contamination (percentage of ISIs < 3 ms), similarity to RSU and FS waveform templates, 60-Hz noise contamination, rise and decay times and slope of the mean waveform, waveform amplitude, and width. Cluster quality was also ensured by thresholding of L-ratio and isolation distance (77). The random forest algorithm classified clusters as noise, multiunit, or single unit. Only single units with a clear refractory period were used for additional analysis. Units were classified as RSU or FS based on the time between the negative peak and the first subsequent positive peak of the mean waveform (Fig. 1*B*). Clusters were classified as RSUs if this value was >0.39 ms and as FS otherwise (19), with a lower threshold of 0.19 ms to eliminate noise. We used previously established criteria and methods to select neurons that we could reliably follow over time (13). Briefly, we considered neurons to be continuously recorded if they satisfied the following criteria: (*i*) waveforms constituting an isolatable cluster, (*ii*) presence of absolute refractory period, (*iii*) minimal change in spike shape across recording days assessed by computing the sum of squared errors between daily average waveforms, (*iv*) high signal-to-noise ratio, and (*v*) stability of firing rate (no continuous increase or

decrease). Only neurons that could be recorded for at least 48 consecutive hours were used for analysis of L-D transitions. For extended dark experiments, we analyzed all neurons that were online for at least 1 h preceding and 1 h following the time of light reexposure. For estimates of mean firing during the extended dark phase, we analyzed the activity of all cells that could be recorded in the first and last 12-h periods during the 60 h of darkness.

Behavioral-State Classification. The behavioral state of animals was classified using a combination of LFP, EMG, and estimate of locomotion based on video analysis (13). LFPs were extracted from 3 separate recorded channels, resampled at 200 Hz, and averaged. The power spectral density was computed in 10-s bins using a fast Fourier transform method (MATLAB "spectrogram" function) using frequency steps of 0.1 Hz from 0.3 to 15 Hz. Power in the delta (0.3 to 4 Hz) and theta (6 to 9 Hz) bands was computed as a fraction of total power in each time bin. A custom algorithm was used to score each 10-s bin and assign 1 of 4 behavioral codes based on the power in each frequency band as well as EMG and movement activity: active wake (high EMG and movement, low delta and theta), quiet wake (low EMG and movement, low delta and theta), rapid eye movement (REM) sleep (very low EMG, no movement, low delta, high theta), and non-rapid eye movement (NREM) sleep (low EMG and movement, high delta, low theta). For each animal, each hour of data was scored separately. The first 10 h were scored manually and used as an initial training set for a random forest classifier (implemented in Python). The classifier was then used to score each successive hour, with manual corrections performed as needed. The classifier was retrained after every hour scored, with a maximum number of 10,000 bins used for training (using only the most recent 10,000 bins).

Extended Darkness, Immunostaining, and Image Analysis. For analysis of c-fos protein after extended darkness, we transferred animals ($n = 13$ rats) to a custom dark box on P21. A light timer was set up to allow for complete control of the L-D cycle inside the box. When animals were P26, lights were allowed to turn off at the regular time (7:30 PM) and set up to not turn back on. Animals were in complete darkness for 60 h from the night of P26 until the night of P28 (ages matched with electrophysiological recordings). On the morning of P29, lights were allowed to turn back on at 7:30 AM. Animals were allowed to experience 1 h of light before being deeply anesthetized and transcardially perfused. Control animals were either not exposed to darkness but kept on a regular 12-h cycle or anesthetized at 7:30 AM on P29 (before lights on) in the dark using infrared night vision goggles and then immediately perfused. Brains were fixed in 3.7% formaldehyde, and 60-μm coronal slices of V1m were taken on a vibratome (Leica VT1000S). Slices were immersed in a solution of phosphate-buffered saline (PBS) and NaN_3 and stored for immunostaining. To ensure consistent results between groups, all conditions were run in parallel. Slices were incubated in a primary antibody solution (1:1,000; rabbit anti–c-fos; Cell Signaling Technologies) at room temperature for 24 h. They were then rinsed and incubated for 2 h with a secondary antibody (anti-rabbit Alexa Fluor 568; 1:400; Thermofisher). Sections were mounted on microscope slides with a DAPI-containing medium (DAPI Fluoromount-G; Southern Biotech), coverslipped, and allowed to dry for 24 h before imaging. Imaging was performed on a confocal microscope (Zeiss Laser Scanning Microscope 880). A 10× objective was used to take *z* stacks of V1m in the DAPI and c-fos channels. Imaging settings were optimized for each staining/imaging session and kept constant across conditions; all conditions were imaged on a given session. Images were imported into Metamorph software for analysis. A granularity analysis was used to determine locations of cell bodies, and colocalized DAPI- and c-fos–positive granules were counted as c-fos–positive neurons. For each slice, we analyzed the whole field of view, excluding the slice edges, as they displayed DAPI staining artifacts.

Analysis of Electrophysiological Data. All electrophysiology data were analyzed using a custom code package written in Python. The precise time of lights on/off was determined by analysis of video recordings or using a light-sensitive resistor. All analyses were performed on the 10 min before and after transitions. Perievent time histograms were obtained by binning data in 0.25-s bins and normalizing data to the pretransition period. Firing rates were estimated by sliding a 1- or 2-min window in 20-s steps. Mean and SEM were estimated by averaging across days. To compare population data across transitions, we calculated the average firing rate in the 10 min before and after the transition without binning. For analysis restricted to a given behavioral state, we only considered transitions during which the animal was in that state for the whole 20 min (10 min before and after the transition). To estimate the number of individual neurons that consistently changed their firing rate in response to L-D and D-L transitions, we used a paired *t* test to determine whether the neuron's firing followed a consistent pattern of change across multiple transitions. We used a bootstrap method to estimate the number of cells expected to pass our significance threshold by chance; for each iteration of the bootstrap, we chose a random time point within the first 24 h. We then created dummy transition times at 12-h intervals from that starting time point and used these dummy transition points to repeat the above analysis for each cell. This procedure was repeated 100 times (i.e., with 100 different dummy transition points) to obtain 100 values for the percentage of significantly changing cells. We used this dataset to estimate the mean and 95% CIs for this parameter. Only neurons that were followed through at least 4 transitions were used for analysis of circadian transitions. For noncircadian transitions, we analyzed neurons that experienced at least 6 transitions.

Pairwise Correlations. Each spike train was binned into spike counts of bin size 100 ms, generating a vector of spike counts for each cell. The spike count correlation coefficient ρ for a pair of neurons was computed in 30-min episodes using a sliding window of 5 min. This produced 139 values for each neuron pair on every single half day (12 h of light and 12 h of darkness). The average of these values then determined the correlation value of each pair for every single half day:

$$\rho_{X,Y} = \frac{E[(X-\mu_X)(Y-\mu_Y)]}{\sigma_X \sigma_Y},$$

where X and Y represent the spike count vectors of 2 cells, respectively; μ_X and μ_Y are the means of X and Y, respectively; σ_X and σ_Y denote the SDs of X and Y, respectively; and E is the expectation. This produced the matrices of pairwise spike count correlations on different half days. To generate the normalized correlation curve, correlations were normalized to the average correlation of each animal at P26 during the light period. Correlations in mixed behavioral states were computed with the above-stated method using the entire 12-h periods of light or dark, while correlations in wake only took into account the wake episodes. Results with bin size of 5 ms followed the same approach.

Experimental Design. Long–Evans rats of both sexes were used throughout all experiments. To estimate the effect of D-L and L-D transitions on firing rates of V1 neurons, we pooled data from previous experiments (13; $n = 7$) as well as newly performed experiments ($n = 4$ rats). Experimental design and timeline were the same across all of these experiments. This dataset was used to produce Figs. 1, 2, 3, and 4. For ISI analyses, we excluded 2 animals for which the precise transition times were known with uncertainty greater than 0.25 s. To analyze the effect of unexpected transitions ($n = 6$ rats) as well as for prolonged darkness experiments ($n = 4$ rats), we used datasets obtained from rats of a similar age (P24 to P35) as those used in analysis of circadian transitions. Electrophysiological data were acquired using the same electrode arrays and recording system in all experiments. For immunohistochemistry experiments, all rats ($n = 13$ animals) were age matched to electrophysiological recordings, and all staining procedures were conducted in parallel across conditions to minimize variability. Slices from all conditions were imaged in every imaging session.

Statistical Analyses. To compare means of 2 populations, we used Wilcoxon rank sum tests. For paired data, both for firing rates and spike count correlations, comparisons were done using a Wilcoxon signed rank test. To compare a population mean to a given value (e.g., 0), we used 1-sample *t* tests for normally distributed data and Wilcoxon signed rank tests for nonnormal distributions. Normality was tested using D'Agostino's K^2 test. To compare cumulative distributions, we used Kolmogorov–Smirnov tests. Data are represented as mean ± SEM. Box plots represent median ± interquartile range, with whiskers extending to the rest of the distribution.

Code Accessibility. All code used for analysis is available from the authors on request.

1. E. Zohary, M. N. Shadlen, W. T. Newsome, Correlated neuronal discharge rate and its implications for psychophysical performance. *Nature* **370**, 140–143 (1994).
2. M. N. Shadlen, W. T. Newsome, The variable discharge of cortical neurons: Implications for connectivity, computation, and information coding. *J. Neurosci.* **18**, 3870–3896 (1998).
3. B. B. Averbeck, P. E. Latham, A. Pouget, Neural correlations, population coding and computation. *Nat. Rev. Neurosci.* **7**, 358–366 (2006).
4. A. Arieli, D. Shoham, R. Hildesheim, A. Grinvald, Coherent spatiotemporal patterns of ongoing activity revealed by real-time optical imaging coupled with single-unit recording in the cat visual cortex. *J. Neurophysiol.* **73**, 2072–2093 (1995).

5. M. Tsodyks, T. Kenet, A. Grinvald, A. Arieli, Linking spontaneous activity of single cortical neurons and the underlying functional architecture. *Science* **286**, 1943–1946 (1999).
6. Y. H. Ch'ng, R. C. Reid, Cellular imaging of visual cortex reveals the spatial and functional organization of spontaneous activity. *Front. Integr. Nuerosci.* **4**, 20 (2010).
7. T. Kenet, D. Bibitchkov, M. Tsodyks, A. Grinvald, A. Arieli, Spontaneously emerging cortical representations of visual attributes. *Nature* **425**, 954–956 (2003).
8. J. Fiser, C. Chiu, M. Weliky, Small modulation of ongoing cortical dynamics by sensory input during natural vision. *Nature* **431**, 573–578 (2004).
9. J. N. MacLean, B. O. Watson, G. B. Aaron, R. Yuste, Internal dynamics determine the cortical response to thalamic stimulation. *Neuron* **48**, 811–823 (2005).
10. A. Luczak, P. Barthó, K. D. Harris, Spontaneous events outline the realm of possible sensory responses in neocortical populations. *Neuron* **62**, 413–425 (2009).
11. A. Luczak, P. Barthó, K. D. Harris, Gating of sensory input by spontaneous cortical activity. *J. Neurosci.* **33**, 1684–1695 (2013).
12. J. L. Gallant, C. E. Connor, D. C. Van Essen, Neural activity in areas V1, V2 and V4 during free viewing of natural scenes compared to controlled viewing. *Neuroreport* **9**, 85–90 (1998).
13. K. B. Hengen, A. Torrado Pacheco, J. N. McGregor, S. D. Van Hooser, G. G. Turrigiano, Neuronal firing rate homeostasis is inhibited by sleep and promoted by wake. *Cell* **165**, 180–191 (2016).
14. K. D. Miller, D. J. MacKay, The role of constraints in Hebbian learning. *Neural Comput.* **6**, 100–126 (1994).
15. G. G. Turrigiano, S. B. Nelson, Homeostatic plasticity in the developing nervous system. *Nat. Rev. Neurosci.* **5**, 97–107 (2004).
16. K. B. Hengen, M. E. Lambo, S. D. Van Hooser, D. B. Katz, G. G. Turrigiano, Firing rate homeostasis in visual cortex of freely behaving rodents. *Neuron* **80**, 335–342 (2013).
17. T. Keck *et al*., Synaptic scaling and homeostatic plasticity in the mouse visual cortex in vivo. *Neuron* **80**, 327–334 (2013).
18. A. K. Dhawale *et al*., Automated long-term recording and analysis of neural activity in behaving animals. *eLife* **6**, e27702 (2017).
19. C. M. Niell, M. P. Stryker, Highly selective receptive fields in mouse visual cortex. *J. Neurosci.* **28**, 7520–7536 (2008).
20. Y. Kawaguchi, Y. Kubota, Correlation of physiological subgroupings of nonpyramidal cells with parvalbumin- and calbindinD28k-immunoreactive neurons in layer V of rat frontal cortex. *J. Neurophysiol.* **70**, 387–396 (1993).
21. L. G. Nowak, R. Azouz, M. V. Sanchez-Vives, C. M. Gray, D. A. McCormick, Electrophysiological classes of cat primary visual cortical neurons in vivo as revealed by quantitative analyses. *J. Neurophysiol.* **89**, 1541–1566 (2003).
22. A. Kohn, Visual adaptation: Physiology, mechanisms, and functional benefits. *J. Neurophysiol.* **97**, 3155–3164 (2007).
23. S. C. Wissig, A. Kohn, The influence of surround suppression on adaptation effects in primary visual cortex. *J. Neurophysiol.* **107**, 3370–3384 (2012).
24. A. Benucci, A. B. Saleem, M. Carandini, Adaptation maintains population homeostasis in primary visual cortex. *Nat. Neurosci.* **16**, 724–729 (2013).
25. K. M. Rosen, M. A. McCormack, L. Villa-Komaroff, G. D. Mower, Brief visual experience induces immediate early gene expression in the cat visual cortex. *Proc. Natl. Acad. Sci. U.S.A.* **89**, 5437–5441 (1992).
26. G. D. Mower, Differences in the induction of Fos protein in cat visual cortex during and after the critical period. *Brain Res. Mol. Brain Res.* **21**, 47–54 (1994).
27. B. Kaminska, L. Kaczmarek, A. Chaudhuri, Visual stimulation regulates the expression of transcription factors and modulates the composition of AP-1 in visual cortex. *J. Neurosci.* **16**, 3968–3978 (1996).
28. L. Kaczmarek, A. Chaudhuri, Sensory regulation of immediate-early gene expression in mammalian visual cortex: Implications for functional mapping and neural plasticity. *Brain Res. Brain Res. Rev.* **23**, 237–256 (1997).
29. D. P. Bartel, M. Sheng, L. F. Lau, M. E. Greenberg, Growth factors and membrane depolarization activate distinct programs of early response gene expression: Dissociation of fos and jun induction. *Genes Dev.* **3**, 304–313 (1989).
30. M. Sheng, G. McFadden, M. E. Greenberg, Membrane depolarization and calcium induce c-fos transcription via phosphorylation of transcription factor CREB. *Neuron* **4**, 571–582 (1990).
31. M. Sheng, M. E. Greenberg, The regulation and function of c-fos and other immediate early genes in the nervous system. *Neuron* **4**, 477–485 (1990).
32. I. V. Kaplan, Y. Guo, G. D. Mower, Immediate early gene expression in cat visual cortex during and after the critical period: Differences between EGR-1 and Fos proteins. *Brain Res. Mol. Brain Res.* **36**, 12–22 (1996).
33. Y. Yamada *et al*., Differential expression of immediate-early genes, c-fos and zif268, in the visual cortex of young rats: Effects of a noradrenergic neurotoxin on their expression. *Neuroscience* **92**, 473–484 (1999).
34. G. D. Mower, I. V. Kaplan, Immediate early gene expression in the visual cortex of normal and dark reared cats: Differences between fos and egr-1. *Brain Res. Mol. Brain Res.* **105**, 157–160 (2002).
35. M. C. D. Bridi *et al*., Two distinct mechanisms for experience-dependent homeostasis. *Nat. Neurosci.* **21**, 843–850 (2018).
36. D. H. Hubel, T. N. Wiesel, Receptive fields of single neurones in the cat's striate cortex. *J. Physiol.* **148**, 574–591 (1959).
37. D. H. Hubel, T. N. Wiesel, Receptive fields, binocular interaction and functional architecture in the cat's visual cortex. *J. Physiol.* **160**, 106–154 (1962).
38. F. W. Campbell, B. G. Cleland, G. F. Cooper, C. Enroth-Cugell, The angular selectivity of visual cortical cells to moving gratings. *J. Physiol.* **198**, 237–250 (1968).
39. J. D. Pettigrew, The effect of visual experience on the development of stimulus specificity by kitten cortical neurones. *J. Physiol.* **237**, 49–74 (1974).
40. G. H. Henry, B. Dreher, P. O. Bishop, Orientation specificity of cells in cat striate cortex. *J. Neurophysiol.* **37**, 1394–1409 (1974).
41. J. A. Movshon, The velocity tuning of single units in cat striate cortex. *J. Physiol.* **249**, 445–468 (1975).
42. R. L. De Valois, E. W. Yund, N. Hepler, The orientation and direction selectivity of cells in macaque visual cortex. *Vision Res.* **22**, 531–544 (1982).
43. M. S. Gizzi, E. Katz, R. A. Schumer, J. A. Movshon, Selectivity for orientation and direction of motion of single neurons in cat striate and extrastriate visual cortex. *J. Neurophysiol.* **63**, 1529–1543 (1990).
44. M. Carandini, D. Ferster, Membrane potential and firing rate in cat primary visual cortex. *J. Neurosci.* **20**, 470–484 (2000).
45. W. E. Vinje, J. L. Gallant, Sparse coding and decorrelation in primary visual cortex during natural vision. *Science* **287**, 1273–1276 (2000).
46. B. Haider *et al*., Synaptic and network mechanisms of sparse and reliable visual cortical activity during nonclassical receptive field stimulation. *Neuron* **65**, 107–121 (2010).
47. R. Herikstad, J. Baker, J. P. Lachaux, C. M. Gray, S. C. Yen, Natural movies evoke spike trains with low spike time variability in cat primary visual cortex. *J. Neurosci.* **31**, 15844–15860 (2011).
48. M. Vinck, R. Batista-Brito, U. Knoblich, J. A. Cardin, Arousal and locomotion make distinct contributions to cortical activity patterns and visual encoding. *Neuron* **86**, 740–754 (2015).
49. M. Dipoppa *et al*., Vision and locomotion shape the interactions between neuron types in mouse visual cortex. *Neuron* **98**, 602–615.e8 (2018).
50. D. M. Berson, F. A. Dunn, M. Takao, Phototransduction by retinal ganglion cells that set the circadian clock. *Science* **295**, 1070–1073 (2002).
51. D. M. Dacey *et al*., Melanopsin-expressing ganglion cells in primate retina signal colour and irradiance and project to the LGN. *Nature* **433**, 749–754 (2005).
52. T. M. Schmidt, P. Kofuji, Functional and morphological differences among intrinsically photosensitive retinal ganglion cells. *J. Neurosci.* **29**, 476–482 (2009).
53. T. M. Brown *et al*., Melanopsin contributions to irradiance coding in the thalamocortical visual system. *PLoS Biol.* **8**, e1000558 (2010).
54. K. E. Davis, C. G. Eleftheriou, A. E. Allen, C. A. Procyk, R. J. Lucas, Melanopsin-derived visual responses under light adapted conditions in the mouse dLGN. *PLoS One* **10**, e0123424 (2015).
55. A. E. Allen, R. Storchi, F. P. Martial, R. A. Bedford, R. J. Lucas, Melanopsin contributions to the representation of images in the early visual system. *Curr. Biol.* **27**, 1623–1632.e4 (2017).
56. A. J. Emanuel, M. T. H. Do, Melanopsin tristability for sustained and broadband phototransduction. *Neuron* **85**, 1043–1055 (2015).
57. A. E. Allen *et al*., Melanopsin-driven light adaptation in mouse vision. *Curr. Biol.* **24**, 2481–2490 (2014).
58. R. P. Rao, D. H. Ballard, Predictive coding in the visual cortex: A functional interpretation of some extra-classical receptive-field effects. *Nat. Neurosci.* **2**, 79–87 (1999).
59. T. Egner, J. M. Monti, C. Summerfield, Expectation and surprise determine neural population responses in the ventral visual stream. *J. Neurosci.* **30**, 16601–16608 (2010).
60. M. G. Shuler, M. F. Bear, Reward timing in the primary visual cortex. *Science* **311**, 1606–1609 (2006).
61. L. Stănişor, C. van der Togt, C. M. Pennartz, P. R. Roelfsema, A unified selection signal for attention and reward in primary visual cortex. *Proc. Natl. Acad. Sci. U.S.A.* **110**, 9136–9141 (2013).
62. C. M. Niell, M. P. Stryker, Modulation of visual responses by behavioral state in mouse visual cortex. *Neuron* **65**, 472–479 (2010).
63. A. Goel, H. K. Lee, Persistence of experience-induced homeostatic synaptic plasticity through adulthood in superficial layers of mouse visual cortex. *J. Neurosci.* **27**, 6692–6700 (2007).
64. M. P. Blackman, B. Djukic, S. B. Nelson, G. G. Turrigiano, A critical and cell-autonomous role for MeCP2 in synaptic scaling up. *J. Neurosci.* **32**, 13529–13536 (2012).
65. Y. Karimipanah, Z. Ma, J. K. Miller, R. Yuste, R. Wessel, Neocortical activity is stimulus- and scale-invariant. *PLoS One* **12**, e0177396 (2017).
66. K. D. Harris, A. Thiele, Cortical state and attention. *Nat. Rev. Neurosci.* **12**, 509–523 (2011).
67. M. L. Schölvinck, A. B. Saleem, A. Benucci, K. D. Harris, M. Carandini, Cortical state determines global variability and correlations in visual cortex. *J. Neurosci.* **35**, 170–178 (2015).
68. D. S. Greenberg, A. R. Houweling, J. N. Kerr, Population imaging of ongoing neuronal activity in the visual cortex of awake rats. *Nat. Neurosci.* **11**, 749–751 (2008).
69. S. Treue, Neural correlates of attention in primate visual cortex. *Trends Neurosci.* **24**, 295–300 (2001).
70. M. Goard, Y. Dan, Basal forebrain activation enhances cortical coding of natural scenes. *Nat. Neurosci.* **12**, 1444–1449 (2009).
71. D. L. Ringach, Spontaneous and driven cortical activity: Implications for computation. *Curr. Opin. Neurobiol.* **19**, 439–444 (2009).
72. A. Destexhe, Intracellular and computational evidence for a dominant role of internal network activity in cortical computations. *Curr. Opin. Neurobiol.* **21**, 717–725 (2011).
73. G. B. Keller, T. Bonhoeffer, M. Hübener, Sensorimotor mismatch signals in primary visual cortex of the behaving mouse. *Neuron* **74**, 809–815 (2012).
74. A. Ayaz, A. B. Saleem, M. L. Schölvinck, M. Carandini, Locomotion controls spatial integration in mouse visual cortex. *Curr. Biol.* **23**, 890–894 (2013).
75. A. B. Saleem, A. Ayaz, K. J. Jeffery, K. D. Harris, M. Carandini, Integration of visual motion and locomotion in mouse visual cortex. *Nat. Neurosci.* **16**, 1864–1869 (2013).
76. K. D. Harris, D. A. Henze, J. Csicsvari, H. Hirase, G. Buzsáki, Accuracy of tetrode spike separation as determined by simultaneous intracellular and extracellular measurements. *J. Neurophysiol.* **84**, 401–414 (2000).
77. N. Schmitzer-Torbert, J. Jackson, D. Henze, K. Harris, A. D. Redish, Quantitative measures of cluster quality for use in extracellular recordings. *Neuroscience* **131**, 1–11 (2005).